A self-blinking DNA probe for live-cell 3D imaging of native chromatin

Yang Zheng[1,2,9], Sen Ye[1,9], Shumin Li[3,9], Cuifang Liu[4,5], Shihang Luo[5,7], Yanqin Chen[2], Yunsheng Li[2], Lingyi Huang[2], Shan Deng[1], Ping Chen[4,8], Yongdeng Zhang[2], Wei Ji[5,7], Ruibang Luo[3], Guohong Li[4,5,6]* & Dan Yang[1,2]*

[1]Morningside Laboratory for Chemical Biology and Department of Chemistry, The University of Hong Kong, Hong Kong, China.

[2]School of Life Sciences, Westlake University, Hangzhou, Zhejiang, China.

[3]Department of Computer Science, The University of Hong Kong, Hong Kong, China.

[4]National Laboratory of Biomacromolecules, CAS Center for Excellence in Biomacromolecules, Institute of Biophysics, Chinese Academy of Sciences, Beijing, China.

[5]College of Life Science, University of Chinese Academy of Sciences, Beijing, China.

[6]Bioland Laboratory (Guangzhou Regenerative Medicine and Health Guangdong Laboratory), Guangzhou, Guangdong, China.

[7]Institute of Biophysics, Chinese Academy of Sciences, Beijing, China

[8]Department of Immunology, School of Basic Medical Sciences, Advanced Innovation Center for Human Brain Protection, Capital Medical University, Beijing, China.

[9]These authors contributed equally: Yang Zheng, Sen Ye, Shumin Li.

*Correspondence: Guohong Li (liguohong@ibp.ac.cn) or Dan Yang (yangdan@westlake.edu.cn)

ABSTRACT

Single-molecule localization microscopy is a powerful superresolution imaging technique to study biological questions by visualizing subcellular fine structures with nanometer-scale precision. However, its application in live-cell imaging studies has been impeded by the paucity of self-blinking organic fluorophores that enable high spatiotemporal resolution and labeling/localization density even at a reduced laser intensity. Herein, we report a self-blinking Si-rhodamine **6-HESiR** and a self-blinking

fluorogenic DNA probe **6-HoeHESiR** developed by structural fine-tuning to suitably increase the "ON" state population. With this chemical probe, we achieved high spatiotemporal resolution and labeling density in the first live-cell 3D superresolution imaging of chromatin fibers with structural polymorphism, even at a modest laser intensity. Selective inhibition of histone deacetylases led to decompaction of chromatin fibers due to hyperacetylation of histones. Our 3D imaging results suggest a model of DNA packaging in interphase with the hierarchical organization of nucleosomal arrays and chromatin fibers.

INTRODUCTION

Superresolution fluorescence microscopy is a powerful tool for interrogating important biological questions. By bypassing the diffraction limit of light, superresolution microscopy has been developed to visualize previously unresolvable fine subcellular structures with nanometer-scale precision[1-6]. However, the best-performing commercial organic dyes (e.g., Alexa 647) widely used for single-molecule localization microscopy (SMLM) still suffer from poor cell permeability and photoswitching buffers that are highly reducing and incompatible with live cells[2,6]. Such limitations have impeded the study of important biological questions by live-cell SMLM. In recent years, self-blinking organic fluorophores such as **HMSiR**[7-10] were developed for SMLM of living cells without using live-cell incompatible photoswitching buffers and 405-nm laser. Yet, high-quality imaging results with high spatiotemporal resolution and labeling density were only achieved in 2D imaging of endoplasmic reticulum (ER)[11] with very high laser intensity[12]. It is still a formidable challenge to achieve high spatiotemporal resolution and labeling density in 3D live-cell SMLM, even at a moderate excitation laser intensity. There is an important principle that the number of "ON" state fluorophores in each frame should be as high as possible to minimize the acquisition time, while it is low enough to avoid PSF overlaps[6]. Currently, a criterion of $pK_{cycl} < 6$ has been adopted for developing self-blinking fluorophores[7-10] without testing those with $pK_{cycl} > 6$. Moreover, there has been no effort to fine-tune the "ON" state population for optimal imaging quality and performance. Therefore, we developed a self-blinking Si-rhodamine

6-HESiR with a suitably increased "ON" fraction by employing the structural fine-tuning strategy[13-15]. By connecting **6-HESiR** to a Hoechst fragment for DNA minor groove binding, we obtained a self-blinking fluorogenic probe **6-HoeHESiR** for imaging native chromatin in living cells. This probe has been validated with *in vitro* reconstituted nucleosomal arrays and 30-nm chromatin fibers, and our 3D imaging results are consistent with EM images. The 3D visualization of both nucleosomal arrays and chromatin fibers in living cells has been achieved with high spatiotemporal resolution and labeling density, even at a reduced laser intensity for lower phototoxicity. We observed structural plasticity of chromatin fibers in both HeLa cells and chicken erythrocytes. Fast chromatin fiber dynamics were captured with less than 2-second temporal resolution, and the mean resting/dwelling lifetime of chromatin fibers was estimated to be 0.6 seconds in HeLa cells and 1 second in chicken erythrocytes. We also observed the decompaction of chromatin fibers induced by small-molecule inhibitors of histone deacetylases (HDACs), providing the first live-cell evidence for the direct link between histone acetylation state and 3D chromatin organization with unprecedented resolution.

RESULTS

The development of a self-blinking fluorogenic DNA probe

To achieve high spatiotemporal resolution and labeling density in 3D live-cell SMLM, we conceived a structural fine-tuning strategy for self-blinking fluorophores with the following criteria: 1) absorption maximum in the deep red and near infrared regions to minimize autofluorescence and phototoxicity to living cells[12] ; 2) a fine-tuned fluorescent "ON" state population for optimal localization number per frame to achieve sufficient labeling density in a short acquisition time while preventing signal overlap[6]; 3) take into account the pH and hydrophobicity that influence the "ON" state population[11]. Based on this new strategy, we developed a self-blinking Si-rhodamine **6-HESiR** (Fig. 1a-b) by installing a hydroxyethyl nucleophile on the upper ring[16,17]. The cyclization/ring opening self-blinking equilibrium is expected to shift toward the open, fluorescent "ON" state. This new fluorophore **6-HESiR** was successfully prepared with an efficient synthetic route (Supplementary Information), and it could

potentially increase the localization number per frame significantly for fast acquisition of sufficient localizations to resolve dynamic fine structures. The "ON" state population of **6-HESiR** was found to be 20% at physiological pH in aqueous buffer with **SiR650** as the benchmark of the 100% "ON" state (Fig. 1b-c, Extended Data Fig. 1), and the pK_{cycl} value of **6-HESiR** was determined to be 6.6 based on its pH titration curve (Fig. 1d), higher than that of **HMSiR** (pK_{cycl} = 5.8, Fig. 1a).

The successful implementation of live-cell SMLM hinges not only on the self-blinking fluorophore but also on a fully biocompatible labeling strategy that is noninvasive, highly selective, and artifact-free with high labeling density. In this regard, we chose the Hoechst tagging strategy[18], as it has found some success in developing fluorogenic probes for live-cell chromatin imaging[18-23] with low cytotoxicity. The Hoechst moiety could perform highly selective noncovalent binding to the DNA minor groove with negligible linkage error between the target DNA molecule and the self-blinking **6-HESiR**. Therefore, we designed and synthesized **6-HoeHESiR** by connecting **6-HESiR** and the Hoechst fragment with a carbamate linker (Fig. 1e). The *in vitro* binding of **6-HoeHESiR** to a benchmark hairpin DNA (hpDNA) molecule (Fig. 1f) with an AATT Hoechst binding site[24] was studied by fluorescence titration. In the absence of hpDNA, the fluorescence of **6-HoeHESiR** was nearly quenched (Fig. 1h). A dose-dependent fluorescence turn-on was observed upon the addition of increasing equivalents of hpDNA to **6-HoeHESiR** (Fig. 1g). A 43-fold fluorescence increase (Fig. 1h) with 14 μM of hpDNA confirmed the sensitivity and fluorogenicity of **6-HoeHESiR**. Based on the titration curve (Fig. 1g), the dissociation constant (K_D) of the complex formed by **6-HoeHESiR** and hpDNA was estimated to be 3.8 μM. Attachment of **6-HESiR** to the Hoechst dye caused a slight redshift of both the absorbance and fluorescence maxima of **6-HoeHESiR** (Extended Data Fig. 2a-b). Upon the addition of hpDNA (14 μM), the absorbance of **6-HoeHESiR** was increased to a level close to that of the free fluorophore **6-HESiR** (Extended Data Fig. 2a), and the fluorescence of **6-HoeHESiR** was recovered to 21% of that of **6-HESiR** (Extended Data Fig. 2b).

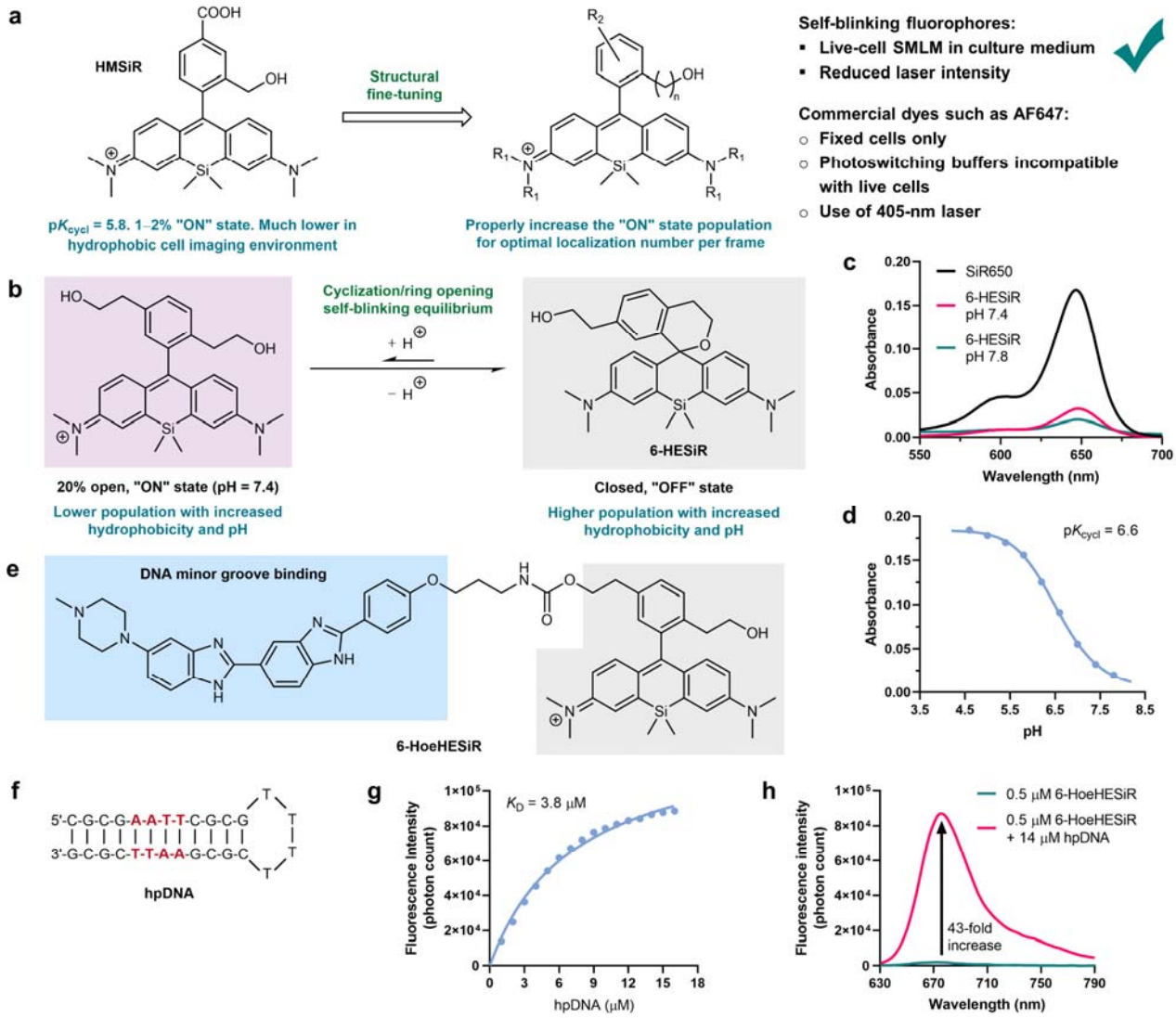

Fig. 1 Development of 6-HESiR and 6-HoeHESiR. a, Structural fine-tuning strategy for developing self-blinking fluorophores. **b**, Self-blinking mechanism. **c**, Absorption spectrum of **6-HESiR** (2 μM) in 0.1 M potassium phosphate buffer (pH = 7.4 and 7.8) with **SiR650** (2 μM) as the "100%" benchmark. Abs_{max} at 648 nm. Fl_{max} at 665 nm. **d**, pH titration of **6-HESiR** (2 μM) in 0.1 M potassium phosphate buffer. **e**, Design of **6-HoeHESiR** by Hoechst tagging strategy. **f**, The hpDNA for fluorescence titration. **g**, Fluorescence titration of **6-HoeHESiR** (0.5 μM) with hpDNA (0–16 μM) in Tris-HCl saline buffer (50 mM Tris-HCl, 100 mM NaCl, pH = 7.4). Fl_{max} at 676 nm. **h**, Fluorescence increases 43-fold in the presence of 14 μM hpDNA.

Validation with lambda DNA and *in vitro* reconstituted chromatin structures

To evaluate our new probe **6-HoeHESiR**, we first attempted an SMLM experiment of spin-coated lambda DNA[25] with $(A/T)_4$ binding sites for the Hoechst moiety[24]. A full width at half maximum (FWHM) of 26 nm was successfully obtained (Extended Data Fig. 3), within the range of 20–30 nm as reported in literature[25]. Then, we focused on *in vitro* reconstituted nucleosomal arrays and 30-nm chromatin fibers as benchmarks well characterized by EM[26] (Fig. 2d and 2f, Extended Data Fig. 4a and 4e). Apart from the AATT binding site, three additional Hoechst binding sites[24] in the DNA template for *in vitro* reconstituted chromatin samples were also identified by fluorescence titration (Fig. 2a, Extended Data Fig. 2c-f). Based on the dissociation constants, the half-life of the complex formed by **6-HoeHESiR** and a nucleosome was estimated to be 10-20 ms[24]. Thus, fast binding/dissociation cycles between **6-HoeHESiR** and nucleosomes could allow fast self-blinking with a pool of **6-HoeHESiR** molecules in the unbound state (Fig. 2b). Since the hydrophobic environment in the nucleus favors the closed "OFF" state[11] (Fig. 1b) and the open form of **6-HoeHESiR** in the unbound state is nearly quenched in fluorescence (Fig. 1h), the "ON" state population of **6-HoeHESiR** in chromatin imaging is expected to be lower than the 20% "ON" fraction of **6-HESiR** measured in aqueous buffer. Gratifyingly, **6-HoeHESiR** exhibited excellent self-blinking in SMLM experiments on reconstituted chromatin samples at a modest laser intensity[12] of 950 W/cm^2 (Supplementary Video 1). The reconstituted nucleosomal arrays displayed the pattern of discrete fluorescence signals (Fig. 2c and 2e, Extended Data Fig. 4b), which resembles the EM images (Fig. 2d, Supplementary Fig. 4a). Analysis of localizations on individual nucleosomes indicated that the ratio of axial to lateral resolution is 2.3 (Extended Data Fig. 4c-d). To extract 3D structural features of reconstituted 30-nm chromatin fibers visualized in 3D SMLM experiments (Fig. 2c and 2g; Extended Data Fig. 4f), we developed an image analysis framework/program (Extended Data Fig. 5-6, Supplementary Information). Statistical results showed that the reconstituted chromatin fibers had a mean diameter of 32 nm, length of 112 nm, mean localization precision of 7.8 nm and labeling density of 31,641 molecules/μm^3 (Fig. 2h, Extended Data Fig. 4g, Supplementary Video 2 and 3). Although the reconstituted 30-nm fibers without biotin labels

were visualized by EM in a dry and flattened state (Supplementary Information), unlike our 3D SMLM approach, the 3D structural features obtained with **6-HoeHESiR** were consistent with those revealed by EM (Fig. 2f-h). Some elongated fibers were observed, probably due to slight loosening in the aqueous buffer (without glutaldehyde as a crosslinker) compared with the dry state in EM analysis.

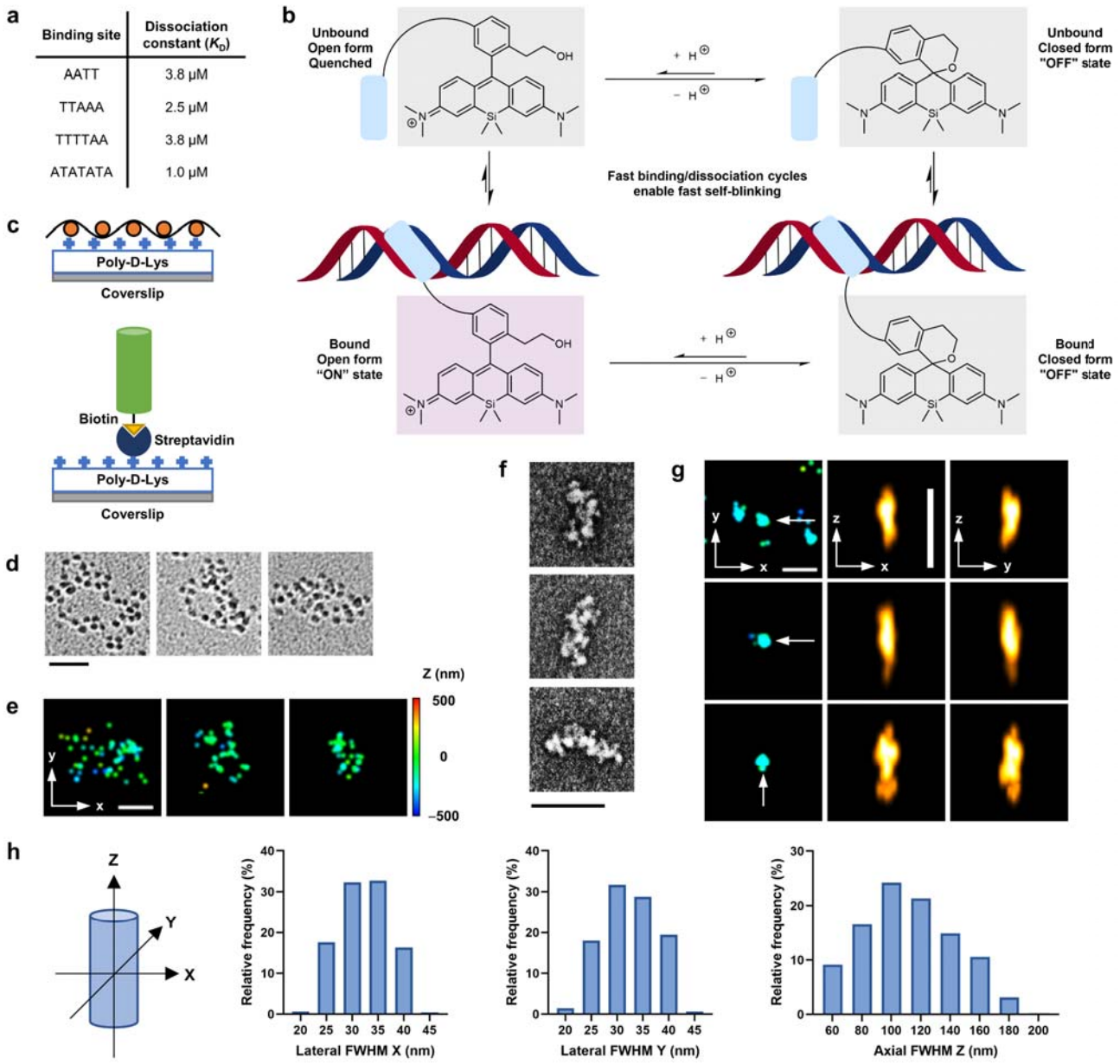

Fig. 2 ***In vitro*** **reconstituted chromatin structures. a**, Dissociation constants of four binding sites in the DNA template. **b**, Working mechanism of **6-HoeHESiR** in the presence of nucleosomes. **c**, Immobilization approaches for 40×187-bp nucleosomal arrays and 30-nm chromatin fibers. **d**, EM

images of nucleosomal arrays. **e**, Images of nucleosomal arrays by 3D SMLM. **f**, EM images of 30-nm chromatin fibers. **g**, Images of 30-nm chromatin fibers by 3D SMLM. 3D sizes by FWHM (x, y, z) in nm (from top to bottom): 27, 29, 81; 26, 30, 93; 30, 30, 101. Localization precision (nm): 6.3, 6, 5.8. **h**, Histograms of 3D sizes of chromatin fibers. N = 483 from 3 fields of view. Incubation with **6-HoeHESiR** (2.5 μM) for 10 min. Scale bar: 100 nm in **d** and **f**; 200 nm in **e** and **g**. Axial position (nm) represented by RGB color depth coding.

Native chromatin 3D structures in living cells

Building upon the solid validation of **6-HoeHESiR** with benchmark *in vitro* reconstituted nucleosomal arrays and 30-nm chromatin fibers, we then attempted to image native chromatin structures in living cells. First, we optimized the incubation conditions of **6-HoeHESiR** with living HeLa cells by light-sheet microscopy (Fig. 3a-b, Extended Data Fig. 7a-b). To our delight, **6-HoeHESiR** exhibited good cell permeability and high selectivity to provide 3D visualization of chromatin structures in whole nuclei. Without the Hoechst fragment, **6-HESiR** did not stain any nuclear component (Extended Data Fig. 7c). Cytotoxicity assay showed that **6-HoeHESiR** caused negligible toxicity with a short incubation time (Extended Data Fig. 7d). Subsequent 3D SMLM experiments showed that **6-HoeHESiR** maintained its excellent self-blinking capacity in living HeLa cells (Supplementary Video 4), and chromatin structures were clearly revealed (Fig. 3c; Extended Data Fig. 8a). Based on the structural resemblance to *in vitro* reconstituted benchmark chromatin samples, we identified two categories of chromatin structures in living HeLa cells. The first category consists of nucleosomal arrays (Fig. 3d), which displayed the same pattern of discrete fluorescence signals (Fig. 2e). The second category consists of chromatin fibers with structural plasticity (Fig. 3e; Extended Data Fig. 8b). With the aid of the same image analysis program, these fibers were identified with a mean localization precision of 7.4 nm, short and long fiber diameters of 33 and 42 nm, and a labeling density of 31,926 molecules/μm^3 (Fig. 3f, Extended Data Fig. 8c, Supplementary Videos 5-6). The statistical distribution of 3D sizes and long-to-short fiber diameter ratios and the heterogeneity of visualized morphologies could reflect the

structural polymorphism of chromatin fibers. Our 2D imaging results are consistent with recent reports[27,28,23] that nucleosome clutches or chromatin domains were observed with no clear evidence of horizontally or randomly oriented chromatin fibers. However, our 3D analysis, performed both manually and by the computer program, identified chromatin fibers oriented axially or slightly tilted from the vertical axis. We propose that such an ordered chromatin fiber orientation might not only be consistent with highly regulated replication and transcription processes but facilitate these processes. The overlay of widefield images showed that the chromatin fibers reside in both the peripheral and the interior regions of the nuclei (Fig. 3g; Extended Data Fig. 6d). Remarkably, native chromatin structures in the nucleus are quite dynamic (Supplementary Video 7). We were able to capture transient chromatin fibers with a temporal resolution of less than 2 seconds (Fig. 3h; Supplementary Video 8). The mean resting/residing lifetime of chromatin fibers was estimated to be 0.6 seconds (Extended Data Fig. 6c), implying fast-turnover transitions that are consistent with fast transcription activities. This dwelling lifetime is comparable to the time scale of folding and unfolding dynamics of *in vitro*-reconstituted 30-nm chromatin fibers revealed by single-molecule force spectroscopy[26]. When the laser intensity was reduced to a modest level of 950 W/cm^2 from 3.2 kW/cm^2 to alleviate phototoxicity, nucleosomal arrays were visualized again, and we could still identify chromatin fibers at sufficient resolution with a mean localization precision of 8.8 nm, short and long fiber diameters of 33 and 42 nm, and a labeling density of 29,436 molecules/μm^3 (Extended Data Fig. 9). Fast chromatin dynamics were also revealed (Supplementary Video 9), and the mean resting lifetime of chromatin fibers was estimated to be 0.6 seconds, consistent with the result obtained at 3.2 kW/cm^2 laser intensity.

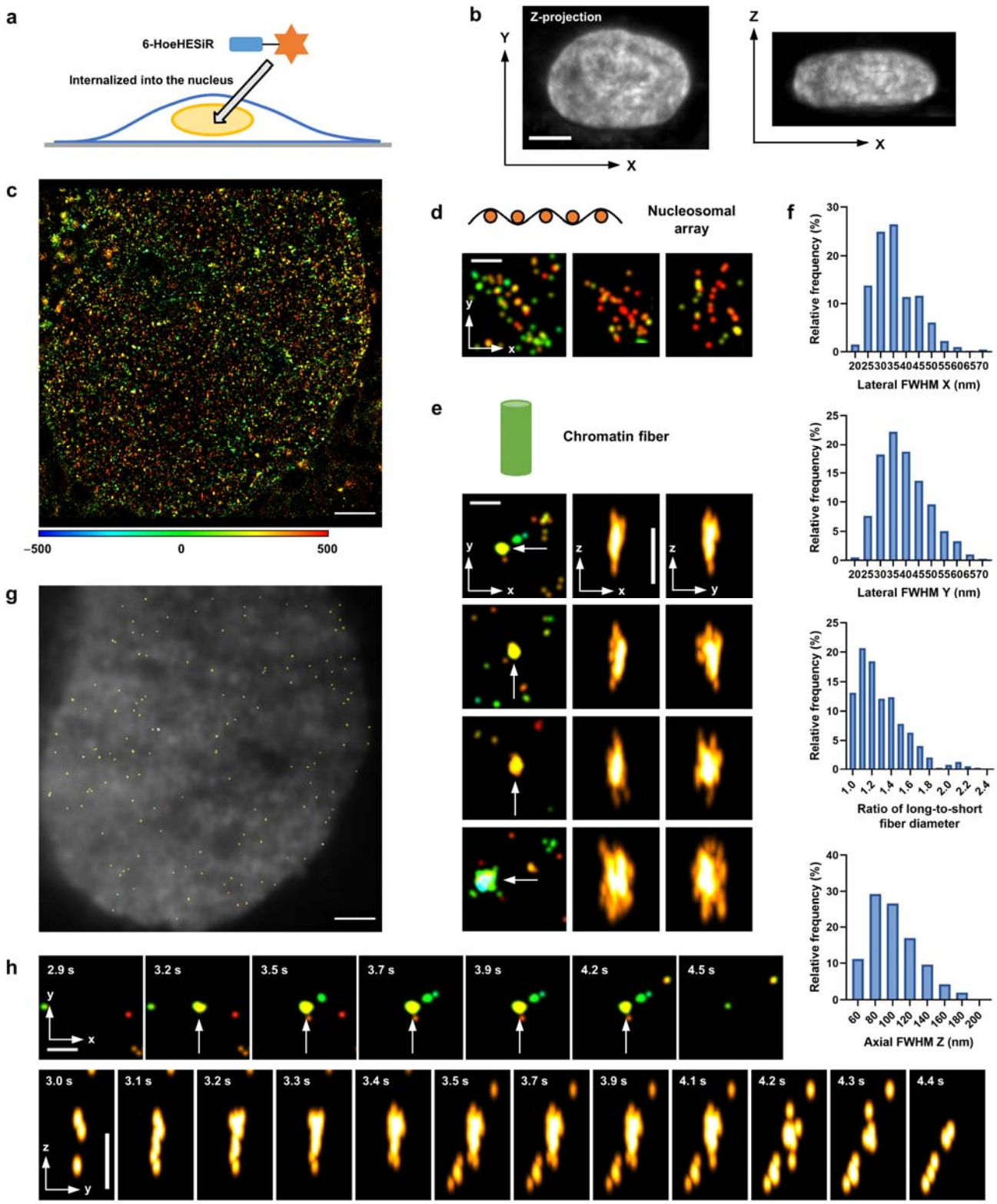

Fig. 3 Native chromatin 3D structures in living HeLa cells. a, Schematic illustration of chromatin labeling with **6-HoeHESiR** (5 μM for 30 min). **b,** Images of a whole nucleus by light-sheet microscopy. **c**, Image of a nucleus. Reconstructed with 2,000 frames (17.7 ms/frame). **d**, Nucleosomal arrays. **e**,

Chromatin fibers. FWHM (x, y, z) in nm (from top to bottom): 30, 30, 107; 35, 42, 124; 34, 51, 102; 69, 51, 154. Localization precision (nm): 7.6, 6.8, 6.8, 9.5. **f**, 3D sizes of chromatin fibers by FWHM. *N* = 396 from 4 cells, identified in 500 frames. **g**, Distribution of chromatin fibers (identified in 500 frames). **h**, Fast dynamics of a chromatin fiber. Snapshots from Supplementary Videos 7 and 8 (Supplementary Information, video legends). Scale bar: 5 µm in **b**; 2 µm in **c** and **g**; 200 nm in **d**, **e** and **h**. Axial position (nm) represented by RGB color depth coding.

A previous cryo-electron tomography (cryo-ET) study identified short chromatin fibers with 30 nm in diameter in isolated nuclei from chicken erythrocytes[29]. Therefore, we also attempted 3D SMLM experiments on living chicken erythrocytes with **6-HoeHESiR**. By applying a modest laser intensity of 950 W/cm^2, 3D chromatin structures in chicken erythrocyte nuclei were successfully visualized (Fig. 4a-c; Extended Data Fig. 10a; Supplementary Video 10). The same two categories of chromatin structures were observed, and chromatin fibers were identified with a mean localization precision of 8 nm, short and long fiber diameters of 29 and 37 nm, and a higher labeling density of 56,359 molecules/µm^3 (Fig. 4d-g; Extended Data Fig. 10b-d; Supplementary Videos 11-12). The fast dynamics of chromatin structures in chicken erythrocyte nuclei were also observed (Supplementary Video 13), with the mean resting lifetime of chromatin fibers estimated to be 1 second.

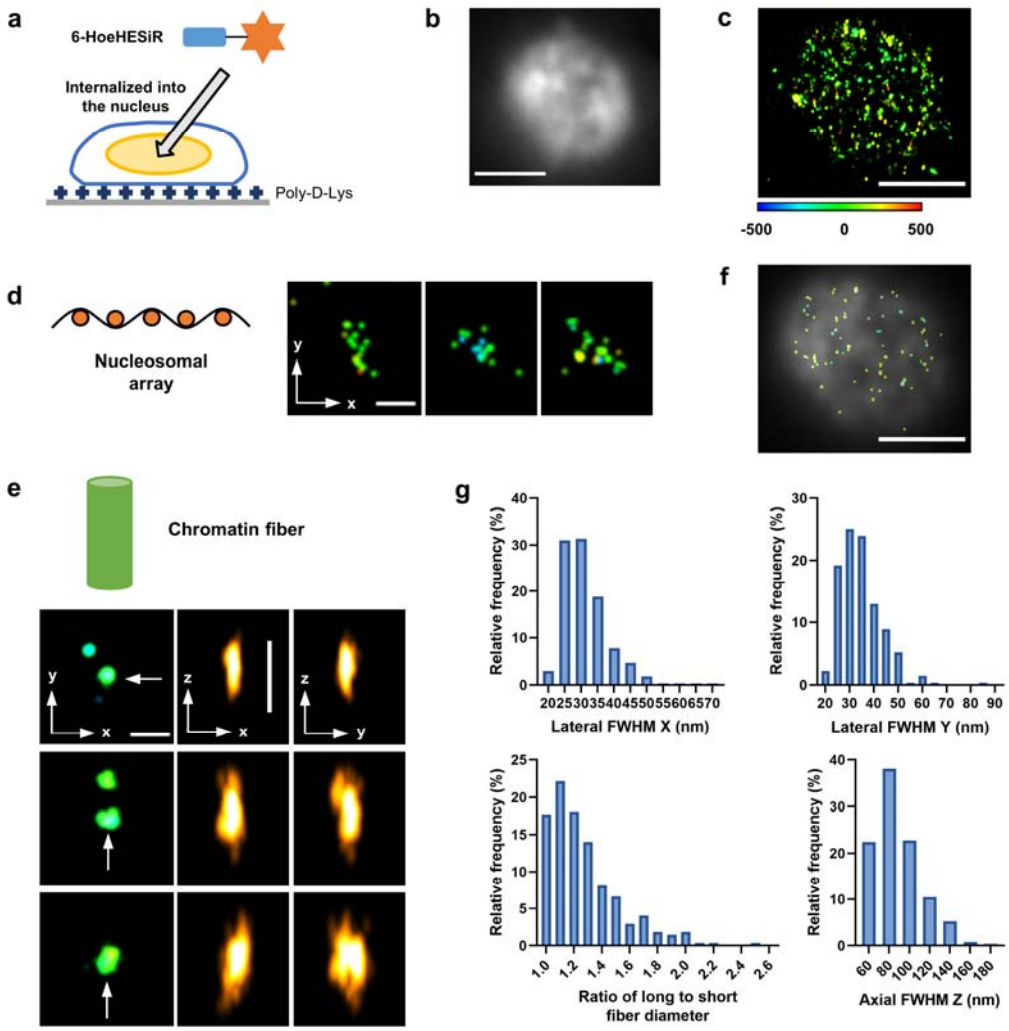

Fig. 4 Native chromatin 3D structures in living chicken erythrocytes. a, Schematic illustration of chromatin labeling with **6-HoeHESiR** (0.5 μM for 10 min). **b,** Image of a nucleus by widefield microscopy. **c**, Image of a nucleus. Reconstructed with 10,000 frames (17.7 ms/frame). **d**, Nucleosomal arrays. **e**, Chromatin fibers. FWHM (x, y, z) in nm (from top to bottom): 27, 29, 83; 37, 40, 124; 40, 62, 95. Localization precision (nm): 6.8, 6.9, 8.1. **f**, 3D sizes of chromatin fibers by FWHM. N = 271 from 3 cells, identified in 5,000 frames. **g**, Distribution of chromatin fibers (identified in 5,000 frames). Scale bar: 2 μm in **b**, **c** and **g**; 200 nm in **d** and **e**. Axial position (nm) represented by RGB color depth coding.

The connection between 3D chromatin organization and histone acetylation

A previous study showed that histone acetylation is a critical epigenetic marker for chromatin fiber relaxation and optimal transcription, while deacetylation is required for chromatin fiber condensation

and transcriptional repression[30]. Histone deacetylases (HDACs), key enzymes that modulate acetylation, can be important drug targets to counteract abnormal protein acetylation status, induce chromatin decompaction, and reactivate tumor suppressor genes[31,32]. To investigate the connection between chromatin fibers and histone acetylation in living cells, we selected three HDAC inhibitors (Fig. 5a): 1) trichostatin A (TSA), a widely used HDAC pan-inhibitor; 2) entinostat, a class I HDAC 1–3 selective inhibitor; and 3) ricolinostat, a class IIb HDAC 6 selective inhibitor. Live HeLa cells were treated with these HDAC inhibitors and then imaged by 3D SMLM (Fig. 5b). The results showed that the density of chromatin fibers decreased by 52% and 63% upon TSA and entinostat treatments, respectively (Fig. 5c-d, Supplementary Fig. 1-2). However, no significant change in fiber density was observed upon ricolinostat treatment (Fig. 5c-d, Supplementary Fig. 3). Both the nonselective inhibition of HDACs and the selective inhibition of class I HDACs 1–3 led to decompaction of chromatin fibers[33,34]. In contrast, selective inhibition of class IIb HDAC 6 induced no significant fiber decompaction. These results are consistent with the literature reports that the functions of class I HDACs 1–3 are exclusively restricted to the nucleus, while class IIb HDAC 6 functions largely outside the nucleus by mediating the deacetylation of cytosolic proteins[35]. Taken together, our live-cell 3D imaging results provide new insights into the global change in 3D chromatin organization in response to histone hyperacetylation induced by small-molecule HDAC inhibitors.

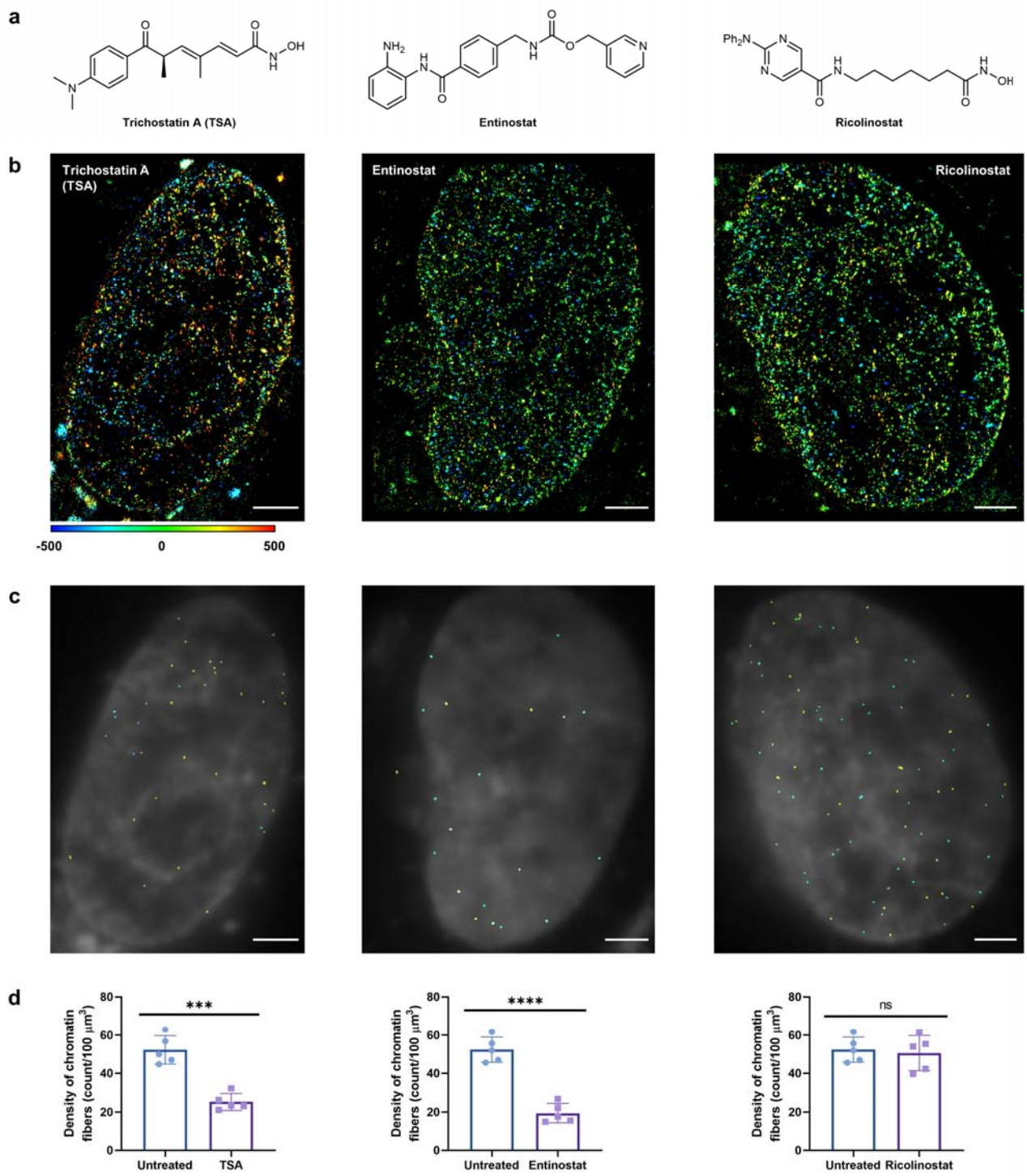

Fig. 5 Decompaction of chromatin fibers induced by HDAC inhibitors. a, Structures of small-molecule inhibitors of HDAC. **b**, Images of the nuclei in treated HeLa cells. Reconstructed with 2,000 frames (17.7 ms/frame). **c**, Distribution of chromatin fibers (identified in 500 frames). **d**, Density of chromatin fibers (identified in 500 frames). Data are individual values and mean ± s.d., N = 5. Statistical significance was determined by *t test* with P = 0.0001, <0.0001 and 0.7278 (from left to right).

The scale bar is 2 μm. Axial position (nm) represented by RGB color depth coding. Cells were treated with TSA (200 nM), entinostat (2 μM), and ricolinostat (1 μM) for 20 h, respectively, and then incubated with **6-HoeHESiR** (5 μM) for 30 min.

DISCUSSION

To conclude, we have demonstrated the success of developing a self-blinking Si-rhodamine **6-HESiR** and a self-blinking fluorogenic DNA probe **6-HoeHESiR** by structurally fine-tuning the "ON" state population to a suitable level. This design strategy has proven effective in 3D imaging of *in vitro* reconstituted chromatin samples and native chromatin in living cells by SMLM. It is noteworthy that high spatiotemporal resolution and labeling density were achieved in live-cell 3D SMLM even at a reduced laser intensity that alleviates phototoxicity. Consequently, we were able to observe native chromatin organized in hierarchical forms of nucleosomal arrays and chromatin fibers with fast dynamics and structural polymorphism. To the best of our knowledge, our 3D imaging results provide the first live-cell evidence for a hierarchical model of native chromatin organization[36-38], through which the 2-m long genomic DNA is highly compacted and packaged into the 10-μm eukaryotic nucleus (Fig. 6). We propose that nucleosomal arrays could be regarded as the primary chromatin structures and chromatin fibers as the secondary and higher-order structures. The structural plasticity/heterogeneity and fast dynamics of chromatin fibers are consistent with the complex regulatory environment in the nucleus, such as histone modifications and variants, nonhistone architectural proteins, and linker DNA lengths for various biological functions[36-38]. The density/population of chromatin fibers was reduced by small-molecule inhibitors of HDACs that are responsible for histone deacetylation. For the first time, this phenomenon provides a live-cell 3D view of the tight connection between the histone acetylation state and chromatin hierarchical organization with unprecedented resolution. In light of our initial success, we anticipate further in-depth studies on the structures and functions of chromatin fibers in DNA-related processes in living cells. We also envision that our structural fine-tuning strategy could be

implemented to develop more self-blinking fluorophores and probes to enable the study of subcellular organelles and biological events by live-cell 3D superresolution imaging.

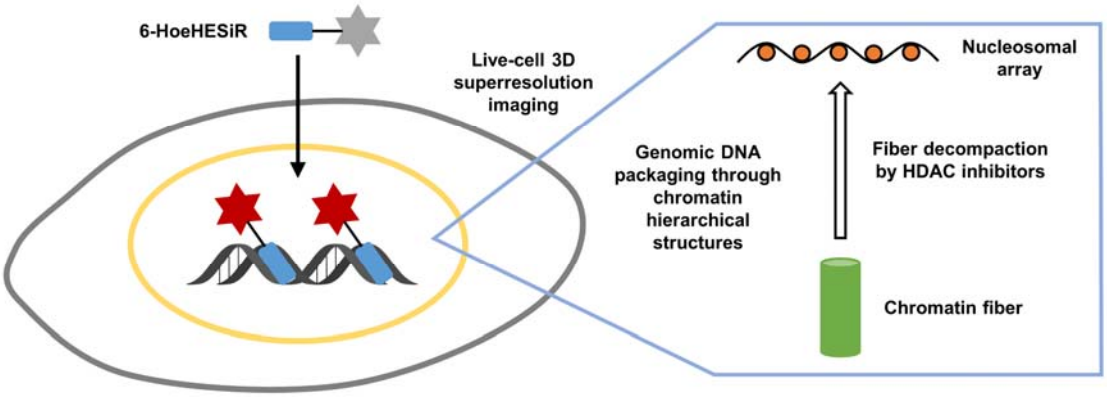

Fig. 6 Schematic illustration of DNA packaging with hierarchical chromatin organization in living cells.

Acknowledgments

We thank the HKU Li Ka Shing Faculty of Medicine Imaging and the Flow Cytometry Core of CPOS for support in cell imaging. This work was supported by The University of Hong Kong, Westlake University, Morningside Foundation, and Hong Kong Research Grants Council under the Area of Excellence Scheme (AoE/P-705/16 to D.Y.). This work was supported by grants for G.L. from the National Natural Science Foundation of China (31991161), the Ministry of Science and Technology of China (2017YFA0504202), the Beijing Municipal Science and Technology Commission (Z201100005320013) and the HHMI International Research Scholars Program (55008737). R. L. was supported by the ECS (grant number 27204518) of the Hong Kong SAR government and by the URC fund at the University of Hong Kong. We thank Ms. Ruiqin Xia for assistance with chemical synthesis and characterization. We thank Dr. Teng Zhao and Dr. Zhe Hu for technical support in light-sheet microscopy. We thank Dr. Zhe Hu, Dr. Teng Zhao, Dr. Shengwang Du and Dr. Wei Li for helpful discussions. We thank Dr. Nai-Kei Wong and Ms. Jasmine Chit Ying Lau for proofreading the manuscript.

Author contributions

Y.Z., G.L. and D.Y. conceived the project. G.L. and D.Y. supervised and directed the research. Y.Z. designed and synthesized **6-HESiR** and **6-HoeHESiR**. Y.Z. studied photophysical properties with contributions from S.Y. C.L. prepared *in vitro*-reconstituted samples and performed electron microscopy analysis. S.-H.L. performed the SMLM experiment with lambda DNA and analyzed the data. Y.Z., S.Y. and S.D. performed cell culture and treatment. Y.Z. and S.Y. performed SMLM experiments with reconstituted chromatin structures and living cells. Y.C. and Y.L. performed the SMLM validation experiments. L.H. performed cytotoxicity assay. S.-M.L. developed the computer program and the web server for chromatin fiber analysis under the supervision of R.L. Y.Z. analyzed chromatin imaging data and performed statistical analysis with contributions from S.Y. and S.-M.L. Y.Z., S.Y., G.L. and D.Y. interpreted imaging results with contributions from all other authors. Y.Z., S.Y., G.L. and D.Y. wrote the manuscript with input from all other authors.

Competing interests

The authors declare no competing interests.

Data availability

All data that support the findings of this manuscript are provided in text, figures, and supplementary videos. Original data are provided upon reasonable request to the correspondence authors.

REFERENCES

1. Liu, Z., Lavis, Luke D. & Betzig, E. Imaging Live-Cell Dynamics and Structure at the Single-Molecule Level. *Mol. Cell* **58**, 644-659 (2015).
2. Sauer, M. & Heilemann, M. Single-Molecule Localization Microscopy in Eukaryotes. *Chem. Rev.* **117**, 7478-7509 (2017).
3. von Diezmann, A., Shechtman, Y. & Moerner, W. E. Three-Dimensional Localization of Single Molecules for Super-Resolution Imaging and Single-Particle Tracking. *Chem. Rev.* **117**, 7244-7275 (2017).

4. Sahl, S. J., Hell, S. W. & Jakobs, S. Fluorescence nanoscopy in cell biology. *Nat. Rev. Mol. Cell Biol.* **18**, 685-701 (2017).
5. Sigal, Y. M., Zhou, R. & Zhuang, X. Visualizing and discovering cellular structures with super-resolution microscopy. *Science* **361**, 880-887 (2018).
6. Lelek, M. *et al.* Single-molecule localization microscopy. *Nat. Rev. Methods Primers* **1**, 39, (2021).
7. Uno, S.-n. *et al.* A spontaneously blinking fluorophore based on intramolecular spirocyclization for live-cell super-resolution imaging. *Nat. Chem.* **6**, 681-689 (2014).
8. Tachibana, R. *et al.* Design of spontaneously blinking fluorophores for live-cell super-resolution imaging based on quantum-chemical calculations. *Chem. Commun.* **56**, 13173-13176 (2020).
9. Chi, W. *et al.* Descriptor ΔGC-O Enables the Quantitative Design of Spontaneously Blinking Rhodamines for Live-Cell Super-Resolution Imaging. *Angew. Chem. Int. Ed.* **59**, 20215-20223 (2020).
10. Tyson, J. *et al.* Extremely Bright, Near-IR Emitting Spontaneously Blinking Fluorophores Enable Ratiometric Multicolor Nanoscopy in Live Cells. *ACS Cent Sci* **7**, 1419-1426 (2021).
11. Takakura, H. *et al.* Long time-lapse nanoscopy with spontaneously blinking membrane probes. *Nat. Biotechnol.* **35**, 773-780 (2017).
12. Wäldchen, S., Lehmann, J., Klein, T., van de Linde, S. & Sauer, M. Light-induced cell damage in live-cell super-resolution microscopy. *Sci. Rep.* **5**, 15348 (2015).
13. Grimm, J. B. *et al.* A general method to fine-tune fluorophores for live-cell and in vivo imaging. *Nat. Methods* **14**, 987-994 (2017).
14. Zheng, Q. *et al.* Rational Design of Fluorogenic and Spontaneously Blinking Labels for Super-Resolution Imaging. *ACS Cent. Sci.* **5**, 1602-1613 (2019).
15. Grimm, J. B. *et al.* A general method to optimize and functionalize red-shifted rhodamine dyes. *Nat. Methods* **17**, 815-821 (2020).

16. Uno, S.-n., Kamiya, M., Morozumi, A. & Urano, Y. A green-light-emitting, spontaneously blinking fluorophore based on intramolecular spirocyclization for dual-colour super-resolution imaging. *Chem. Commun.* **54**, 102-105 (2018).
17. Butkevich, A. N. Modular Synthetic Approach to Silicon-Rhodamine Homologues and Analogues via Bis-aryllanthanum Reagents. *Org. Lett.* **23**, 2604-2609 (2021).
18. Nakamura, A. *et al.* Hoechst tagging: a modular strategy to design synthetic fluorescent probes for live-cell nucleus imaging. *Chem. Commun.* **50**, 6149-6152 (2014).
19. Lukinavičius, G. *et al.* SiR–Hoechst is a far-red DNA stain for live-cell nanoscopy. *Nat. Commun.* **6**, 8497 (2015).
20. Bucevičius, J., Keller-Findeisen, J., Gilat, T., Hell, S. W. & Lukinavičius, G. Rhodamine–Hoechst positional isomers for highly efficient staining of heterochromatin. *Chem. Sci.* **10**, 1962-1970 (2019).
21. Zhang, X. *et al.* A targetable fluorescent probe for dSTORM super-resolution imaging of live cell nucleus DNA. *Chem. Commun.* **55**, 1951-1954 (2019).
22. Bucevičius, J., Kostiuk, G., Gerasimaitė, R., Gilat, T. & Lukinavičius, G. Enhancing the biocompatibility of rhodamine fluorescent probes by a neighbouring group effect. *Chem. Sci.* **11**, 7313-7323 (2020).
23. Bucevičius, J., Gilat, T. & Lukinavičius, G. Far-red switching DNA probes for live cell nanoscopy. *Chem. Commun.* **56**, 14797-14800 (2020).
24. Breusegem, S. Y., Clegg, R. M. & Loontiens, F. G. Base-sequence specificity of Hoechst 33258 and DAPI binding to five $(A/T)_4$ DNA sites with kinetic evidence for more than one high-affinity Hoechst 33258-AATT complex. *J. Mol. Biol.* **315**, 1049-1061 (2002).
25. Zhang, Y. *et al.* Ultrafast, accurate, and robust localization of anisotropic dipoles. *Protein & Cell* **4**, 598-606 (2013).

26. Li, W. *et al.* FACT Remodels the Tetranucleosomal Unit of Chromatin Fibers for Gene Transcription. *Mol. Cell* **64**, 120-133 (2016).
27. Ricci, Maria A., Manzo, C., García-Parajo, M. F., Lakadamyali, M. & Cosma, Maria P. Chromatin Fibers Are Formed by Heterogeneous Groups of Nucleosomes In Vivo. *Cell* **160**, 1145-1158 (2015).
28. Nozaki, T. *et al.* Dynamic Organization of Chromatin Domains Revealed by Super-Resolution Live-Cell Imaging. *Mol. Cell* **67**, 282-293 (2017).
29. Scheffer, M. P., Eltsov, M. & Frangakis, A. S. Evidence for short-range helical order in the 30-nm chromatin fibers of erythrocyte nuclei. *Proc. Natl. Acad. Sci. U.S.A.* **108**, 16992-16997 (2011).
30. Li, G. *et al.* Highly Compacted Chromatin Formed In Vitro Reflects the Dynamics of Transcription Activation In Vivo. *Mol. Cell* **38**, 41-53 (2010).
31. Li, Y. & Seto, E. HDACs and HDAC Inhibitors in Cancer Development and Therapy. *Cold Spring Harb. Perspect. Med.* **6**, a026831 (2016).
32. Eckschlager, T., Plch, J., Stiborova, M. & Hrabeta, J. Histone Deacetylase Inhibitors as Anticancer Drugs. *Int. J. Mol. Sci.* **18**, 1414 (2017).
33. Tóth, K. F. *et al.* Trichostatin A-induced histone acetylation causes decondensation of interphase chromatin. *J. Cell Sci.* **117**, 4277-4287 (2004).
34. Otterstrom, J. *et al.* Super-resolution microscopy reveals how histone tail acetylation affects DNA compaction within nucleosomes in vivo. *Nucleic Acids Res.* **47**, 8470-8484 (2019).
35. Fallah, M. S., Szarics, D., Robson, C. M. & Eubanks, J. H. Impaired Regulation of Histone Methylation and Acetylation Underlies Specific Neurodevelopmental Disorders. *Front. Genet.* **11**, 613098 (2021).
36. Li, G. & Reinberg, D. Chromatin higher-order structures and gene regulation. *Curr. Opin. Genet. Dev.* **21**, 175-186 (2011).

37. Luger, K., Dechassa, M. L. & Tremethick, D. J. New insights into nucleosome and chromatin structure: an ordered state or a disordered affair? *Nat. Rev. Mol. Cell Biol.* **13**, 436-447 (2012).

38. Chen, P., Li, W. & Li, G. Structures and Functions of Chromatin Fibers. *Annual Review of Biophysics* **50**, 95-116 (2021).

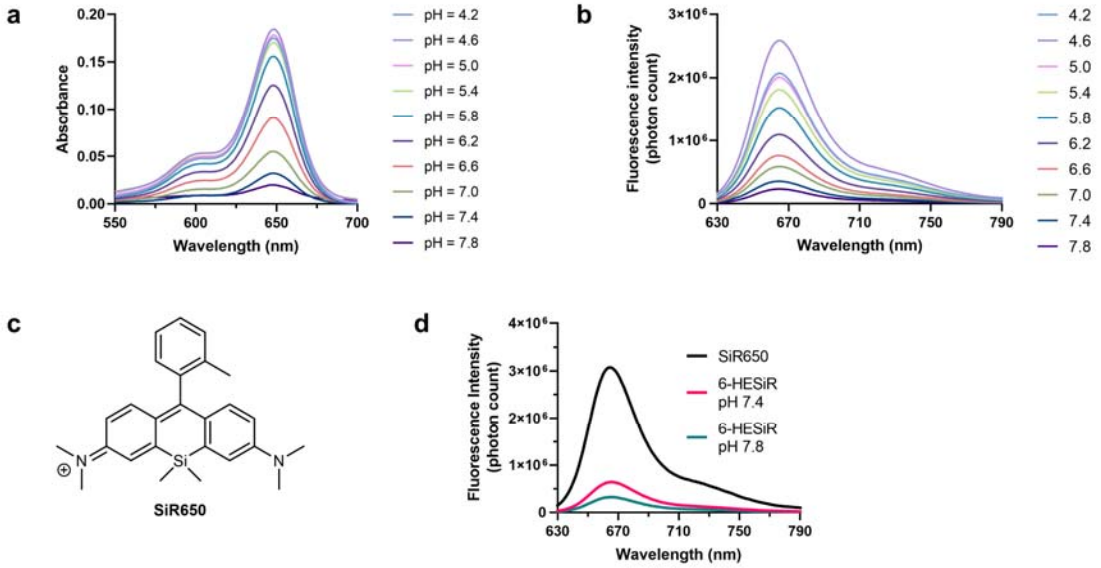

Extended Data Fig. 1 Photophysical properties of 6-HESiR. a, Absorption spectra of **6-HESiR** (2 μM) at various pH values in 0.1 M potassium phosphate buffer. **b**, Fluorescence emission spectra of **6-HESiR** (0.5 μM) at various pH values in 0.1 M potassium phosphate buffer. **c**, Structure of **SiR650**. **d**, Fluorescence emission spectra of **6-HESiR** (2 μM) in 0.1 M potassium phosphate buffer (pH = 7.4 and 7.8) with **SiR650** (2 μM) as the "100%" benchmark.

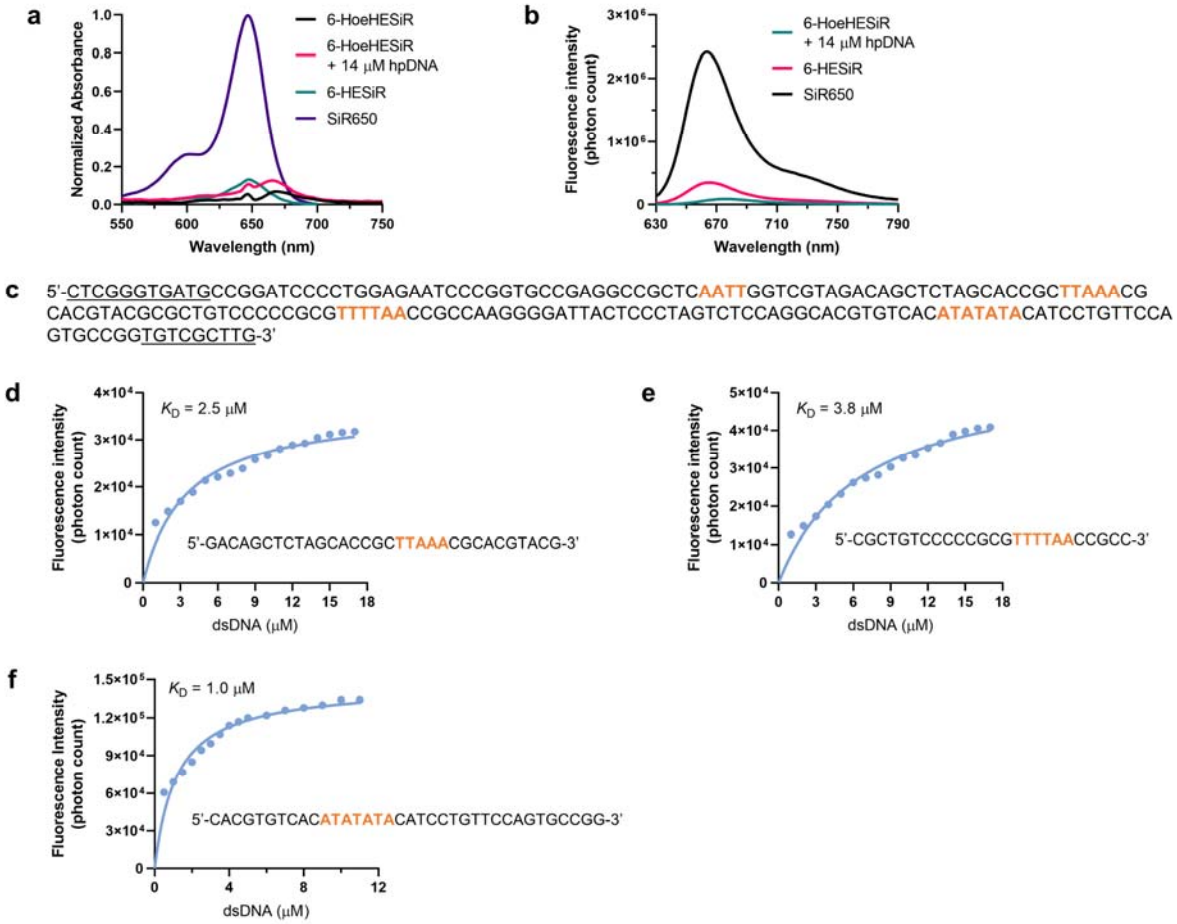

Extended Data Fig. 2 Fluorescence titration of 6-HoeHESiR. a, Absorbance of **6-HoeHESiR** (0.5 μM) in Tris-HCl saline buffer (50 mM Tris-HCl, 100 mM NaCl, pH = 7.4). **b**, Fluorescence of **6-HoeHESiR**, **6-HESiR** and **SiR650** (0.5 μM) in Tris-HCl saline buffer. **c**, Sequence of the 187-bp DNA template for reconstituted chromatin samples. The linker DNA sequence is underlined. **d-f**, Fluorescence titration with 0.5 μM **6-HoeHESiR** and dsDNA segments in the Tris-HCl saline buffer.

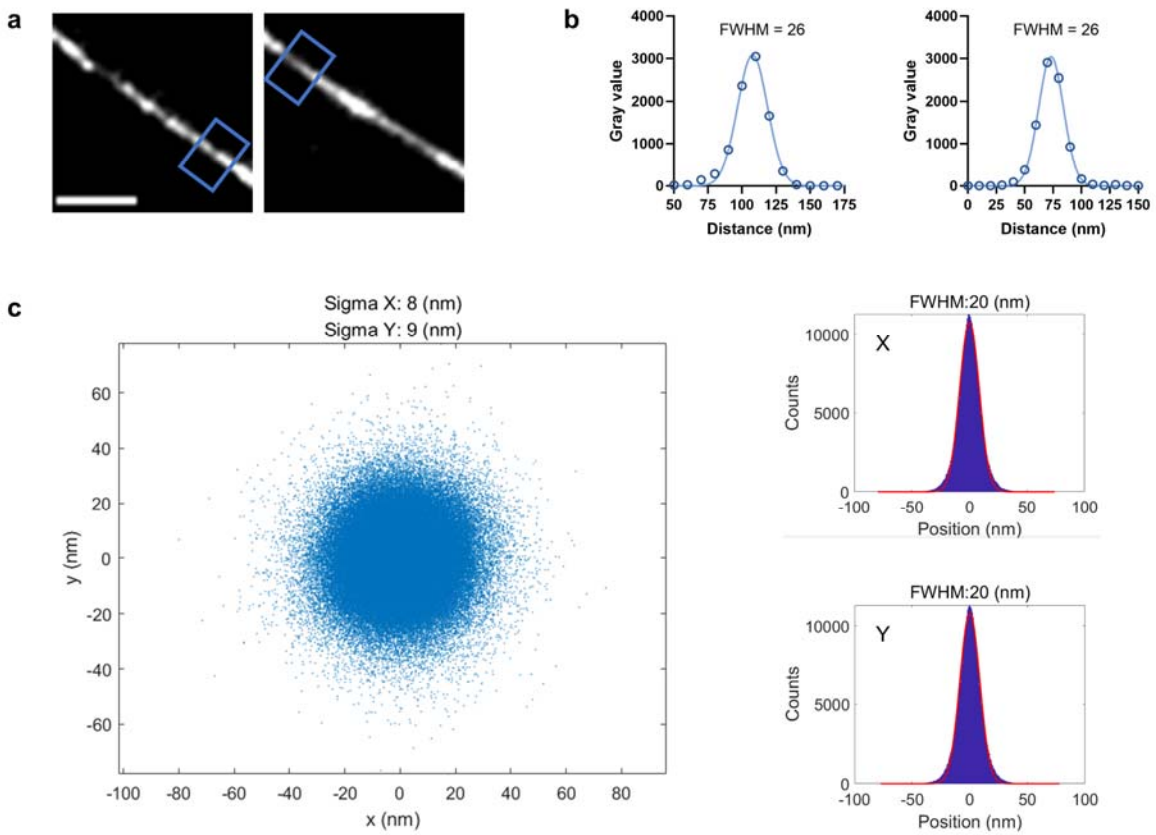

Extended Data Fig. 3 SMLM with lambda DNA. a, Reconstructed images of spin-coated λ-DNA. **b**, Line profiles for the boxed regions in **a** for obtaining FWHM values. **c**, Localization precision. Imaging performed with 100 nM **6-HoeHESiR**. Scale bar: 200 nm.

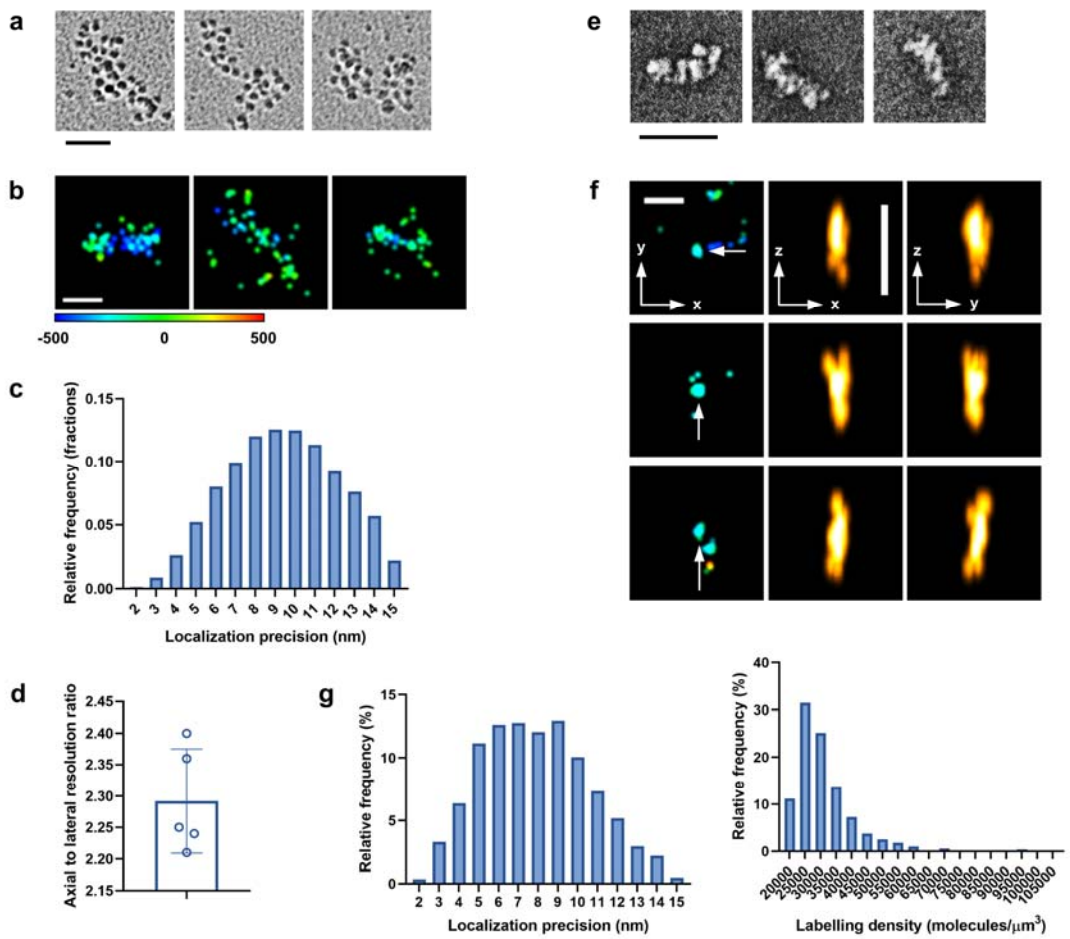

Extended Data Fig. 4 SMLM with *in vitro* reconstituted chromatin structures. a, EM images of 40×187-bp nucleosomal arrays (by metal-shadowing). **b**, Images of 40×187-bp nucleosomal arrays by 3D SMLM. **c**, Localization precision for 40×187-bp nucleosomal arrays. **d**, Ratio of axial resolution to lateral resolution. Data are mean ± s.d., N = 5. **e**, EM images of 40×187-bp 30-nm chromatin fibers (by negative staining). **f**, Images of 40×187-bp 30-nm fibers by 3D SMLM. FWHM (x, y, z) in nm (from top to bottom): 25, 30, 88; 27, 29, 95; 29, 33, 107. Localization precision (nm): 4.3, 6.8, 5.9. **g**, Localization precision and labeling density for identified 30-nm chromatin fibers. Incubation with **6-HoeHESiR** (2.5 μM) for 10 min. Scale bar: 100 nm in **a** and **e**; 200 nm in **b** and **f**. Axial position (nm) represented by RGB color depth coding.

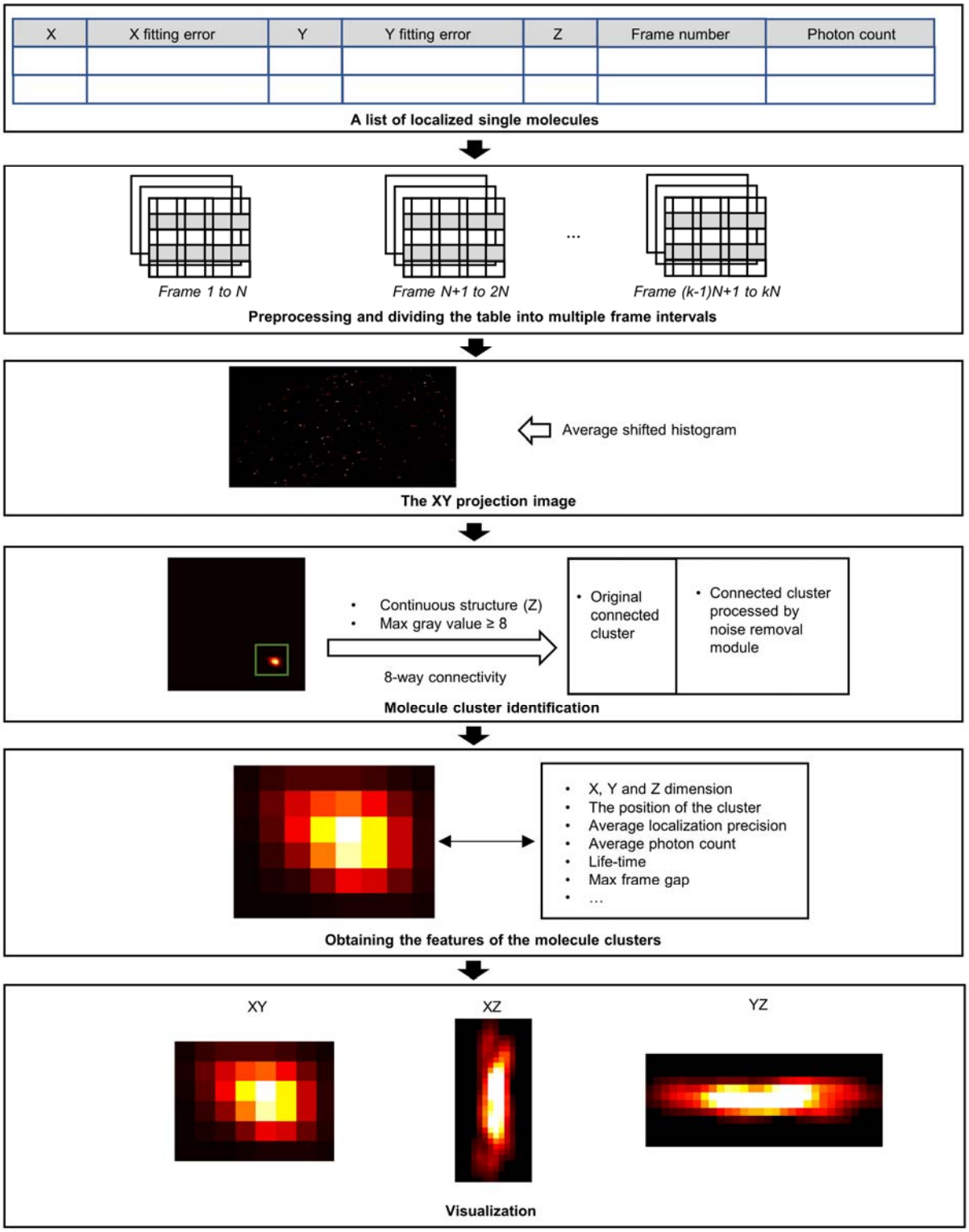

Extended Data Fig. 5 The flowchart of the analysis of molecular clusters for identification of chromatin fibers.

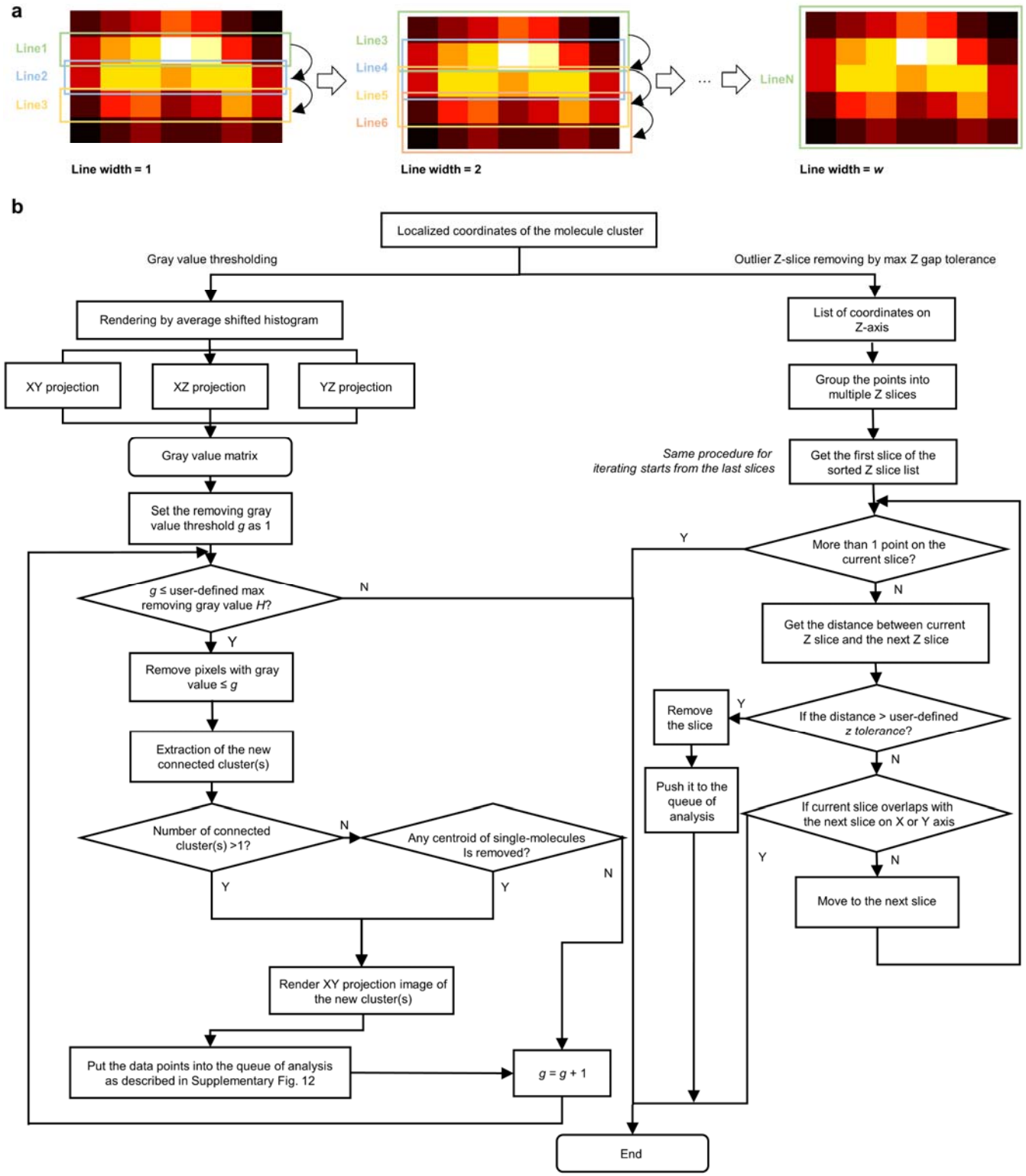

Extended Data Fig. 6 Chromatin fiber analysis program. a, The demonstration of the moving line strategy for estimating X dimension of molecular clusters. **b**, The flowchart of the noise removal module, which consists of two submodules: gray value thresholding and outlier Z slice removing by max Z gap tolerance. *g* ranges from 1 to the user-defined max threshold *H*.

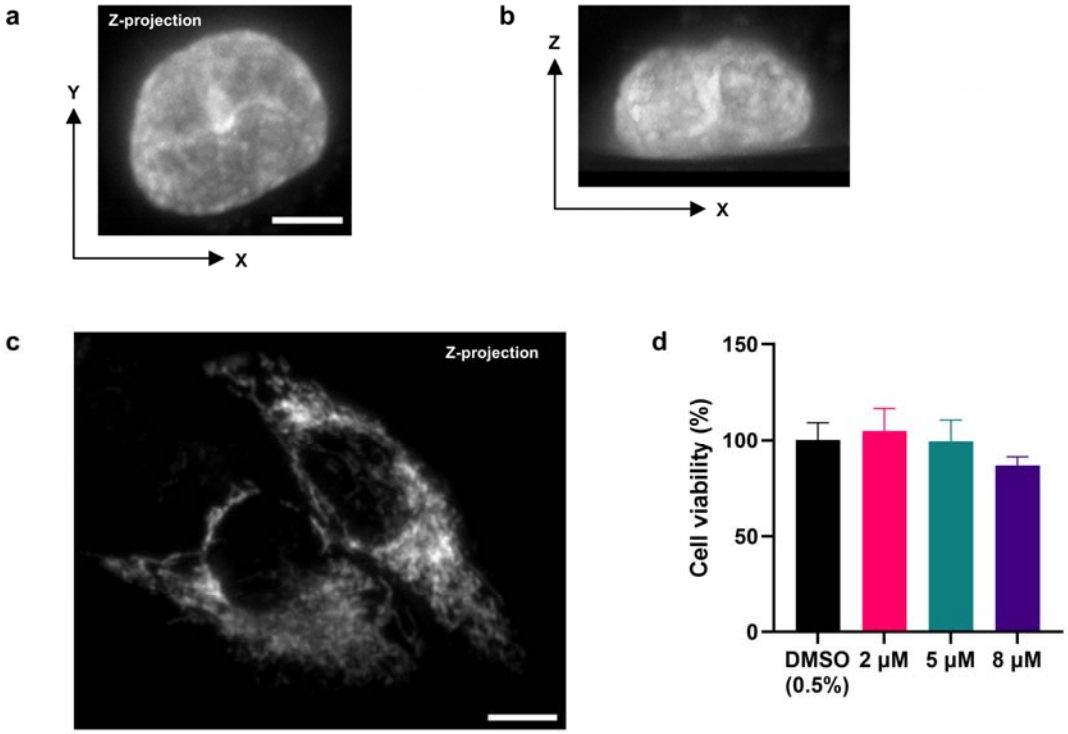

Extended Data Fig. 7 Light-sheet microscopy of living HeLa cells. a, The Z-projection image of the nucleus in a living HeLa cell. **b,** The XZ projection image of the same nucleus. **c**, The Z-projection image of living HeLa cells stained with **6-HESiR**. **d**, Cytotoxicity assay with **6-HoeHESiR** (5 h incubation in DMEM). *N* = 3, data are mean + SD. Incubation with **6-HoeHESiR** (**a** and **b**, 5 μM) and **6-HESiR** (**c**, 2 μM) for 30 min, respectively. Scale bar: 5 μm in **a** and **b**; 10 μm in **c**.

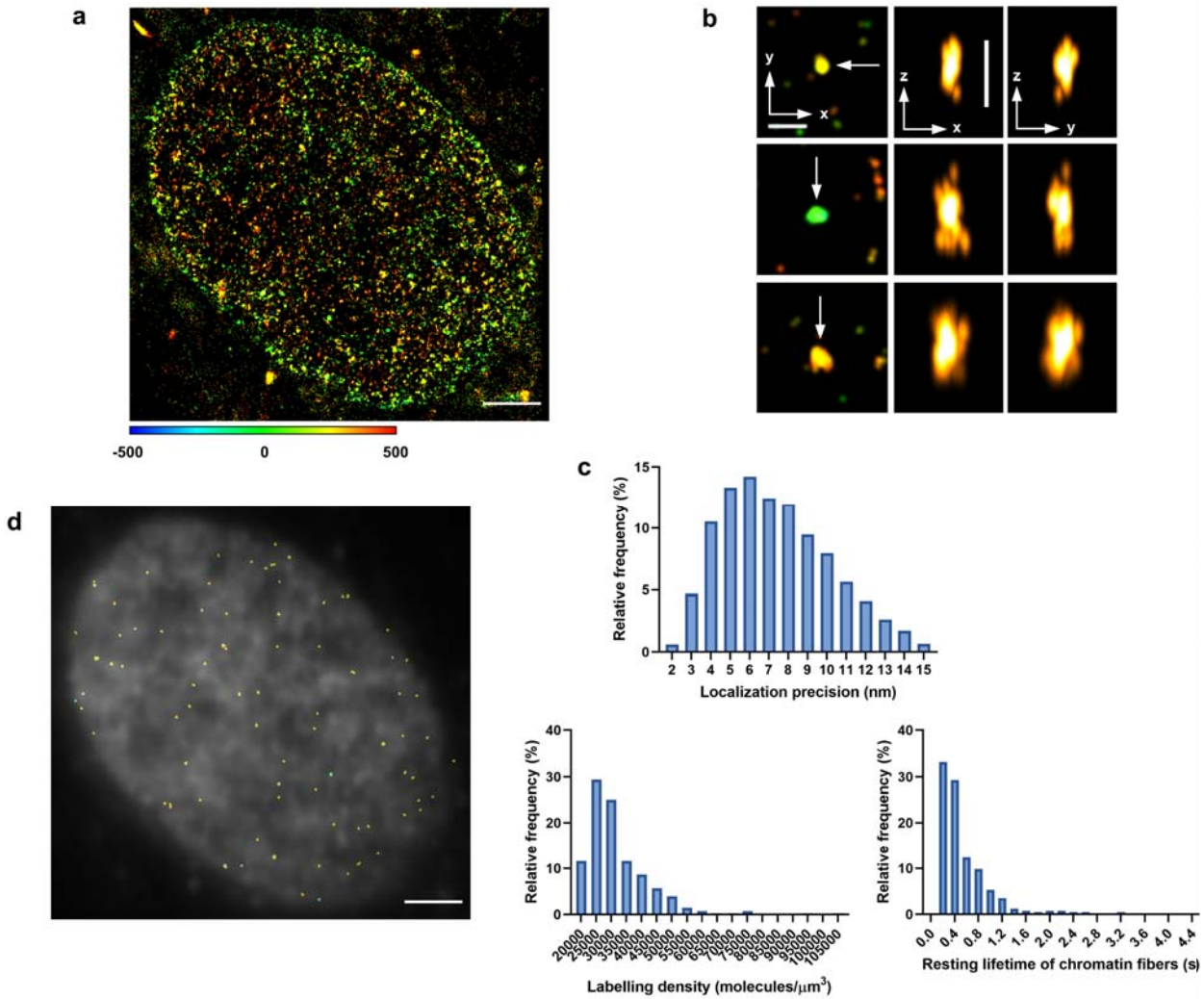

Extended Data Fig. 8 Chromatin fibers in living HeLa cells. a, The image of a nucleus. Reconstructed from 2,000 frames (17.7 ms/frame). **b**, High-order chromatin fibers. FWHM (x, y, z) in nm (from top to bottom.): 31, 34, 94; 44, 35, 116; 45, 50, 103. Localization precision (nm): 7, 7.2, 9.1. **c**, Localization precision, labeling density, and resting lifetime for identified fibers in 500 frames. **d**, The distribution of chromatin fibers (identified in 500 frames). Incubation with **6-HoeHESiR** (5 μM) for 30 min. Scale bar: 2 μm in **a** and **d**; 200 nm in **b**. Axial position (nm) represented by RGB color depth coding.

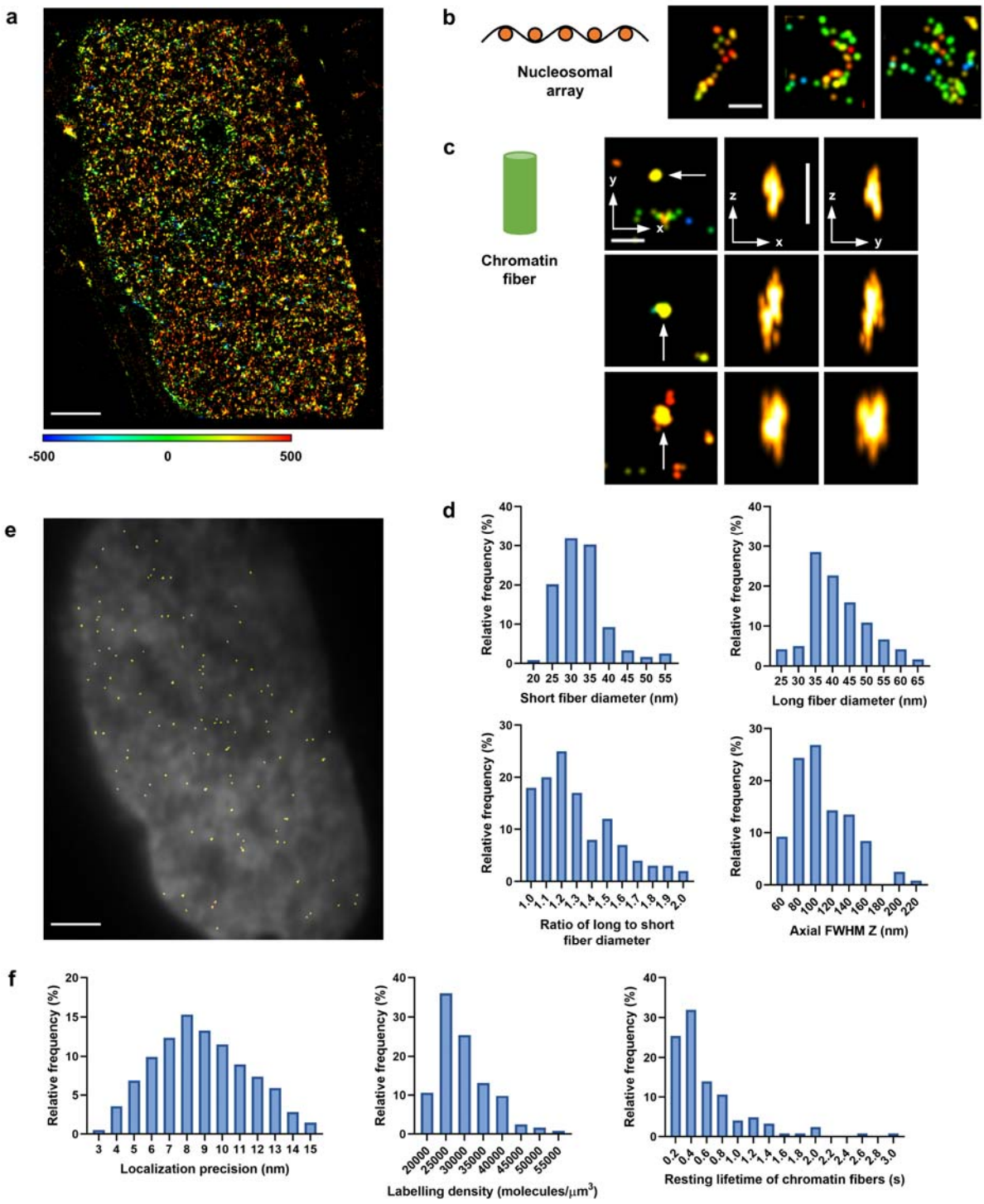

Extended Data Fig. 9 Native chromatin 3D structures revealed with reduced phototoxicity. a, The image of the nucleus in a live HeLa cell. Reconstructed from 2,000 frames (17.7 ms/frame). **b**, Images of nucleosomal arrays. **c**, Chromatin fibers. FWHM (x, y, z) in nm (from top to bottom): 31, 33, 95; 42, 36, 130; 47, 62, 112. Localization precision (nm): 6.8, 7.2, 8.9. **d**, 3D sizes of identified fibers in 500 frames. N = 119. **e**, The distribution of chromatin fibers (identified in 500 frames). **f**, Localization

precision, labeling density, and resting lifetime for identified fibers in 500 frames. Incubation with **6-HoeHESiR** (5 μM) for 30 min. Scale bar: 2 μm in **a** and **e**; 200 nm in **b** and **c**. Axial position (nm) represented by RGB color depth coding.

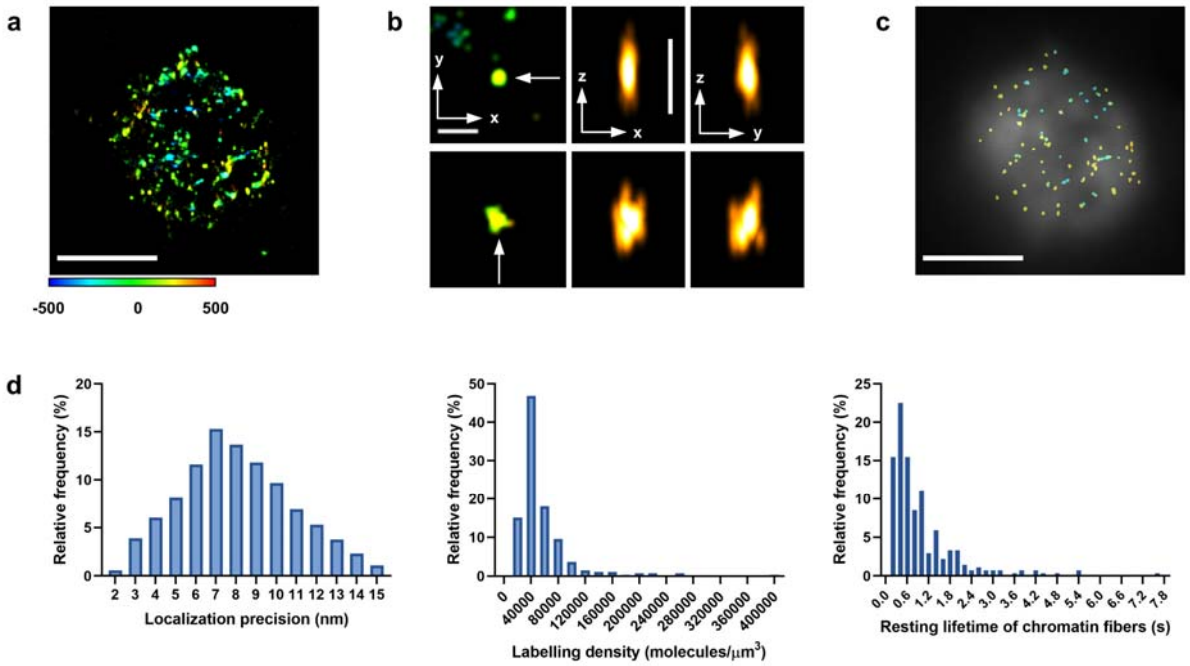

Extended Data Fig. 10 Chromatin fibers in living chicken erythrocytes. a, The image of a nucleus. Reconstructed with 5,000 frames (17.7 ms/frame). **b**, Chromatin fibers. FWHM (x, y, z) in nm (upper, lower): 25, 33, 84; 51, 47, 94. Localization precision (nm): 7.4, 8.5. **c**, The distribution of chromatin fibers (data from 5,000 frames). **d**, Localization precision, labeling density, and resting lifetime for identified fibers in 5,000 frames. Incubation with **6-HoeHESiR** (0.5 μM) for 10 min. Scale bar: 2 μm in **a** and **c**; 200 nm in **b**. Axial position (nm) represented by RGB color depth coding.